Version 1.1

Pg 150 Glasers Annalen July 1952

MATHEMATICAL-GRAPHIC METHOD FOR THE CALCULATION OF RIGID STAYBOLTS WITH NEW DESIGN SHAFTS UNDER ALL POSSIBLE DEMANDS AND CONDITIONS

Von Dr. Ing. Arnold Tross

Translated By: Inge von Kehl, Clinical Toxicologist, ret.
Edited by: Cynthia Meister, M.S. English Literature
Matt Janssen, CEO, Vapor Locomotive Company
2006

(Introductory note, not translated.)

1) THE BENDING FACTOR M AND THE ANGLE FACTOR M'

These derived formulas are only valid for rigid cylindrical shafts (BgD), staybolts with preformed, that is staybolts with an old head, but with a new design shaft, where the ending factor m and the angle factor m' must be considered. The bending factor m yields a significant number, which describes how many times the axis of the staybolts with a diameter of D_E of a new design shaft compares with the bending factor of a staybolt of the same diameter D_E (BgD). This factor m is important, expressing the permissible degree of bending of the staybolt with a particular type of construction and characteristic material. With the help of the Mohrishe Skylift process this can be put into a graphic display. The bending factor m

$$m = \frac{f_{bBmvS}}{f_{bBgD}} \qquad (65)$$

where f_{bBgD} and f_{bBmvS} is the arrow of direction of the bend of the staybolt with a cylindrical shaft as an example, the New Design shaft which has the same capacity of bending and diameter. However, by bending to a higher degree, angle β does not always follow in direct proportion.
Therefore, the angle factor m' becomes

$$m' = \frac{\beta_{BmvS}}{\beta_{bBgD}} \qquad (66)$$

This equation indicates by how much larger the bending power Q will be with a new design staybolt but with the same angle β and by a larger BgD.

The difference between angle and bending factor is expressed in:

$$m'' = \frac{m'}{m} \tag{67}$$

This will yield the information of how many formulations are used in order to determine the value β when utilizing a new design staybolt. One also must consider the enlarged bending direction (arrow).

The factors m, m' and m" must be determined independently for each altered condition for each staybolt in order to obtain a clear understanding of the bending capacity. This in turn will yield:

m_{sF}, m'_{sF}, and m''_{sF},

In the case of pure bend with m_{rB}, m'_{rB}, m''_{rB} and in the case of bending only free staybolts, the values change to

m_{fF}, m'_{fF} and m''_{fF}.

In ordinary conditions ($\delta = 0$) the values can then be reduced to simply:

m_n, m'_n and m''_n.

From eq 52, 56 and 61 it is known that the angle β becomes independent of the angle γ and in three special situations the relationship becomes 1.5: 2: 3. Employing the Mohrishe Skylift principle one will be able to determine the bending factor m (Ill. 12) under the three special cases 1.5: 2: 3, and at the same time take note that all will be on the same straight line. Continuing on the same straight line until the Y-axis, one will obtain the bending factor $\beta = 0$. Dealing with new design shafts only, the line of bending will be altered. Excluding the anchor angles β' and γ' the application forces M_{Bfs} and M_{Bss} depend on the bending factor $\beta = 0$, and also the demand forces $\delta = 0$. One can obtain this information from (Ill. 12) which provides the following relationship:

$$m_{rB} = \frac{m_{fF} + 2\, m_{sF}}{3} \tag{68}$$

$$m_{fF} = 3\, m_{rB} - 2\, m_{sF} \tag{69}$$

$$m_n = 2\, m_{sf} - m_{fF} \tag{70}$$

In addition one can use these equations to determine other values such as:

$$m'_{sF} = m_{rB} \tag{71}$$

and the case of perfect symmetrical staybolts the length of the head:

$$m'_{sF} = m'_{rB} = m'_{fF} = m_{rB}. \qquad (72)$$

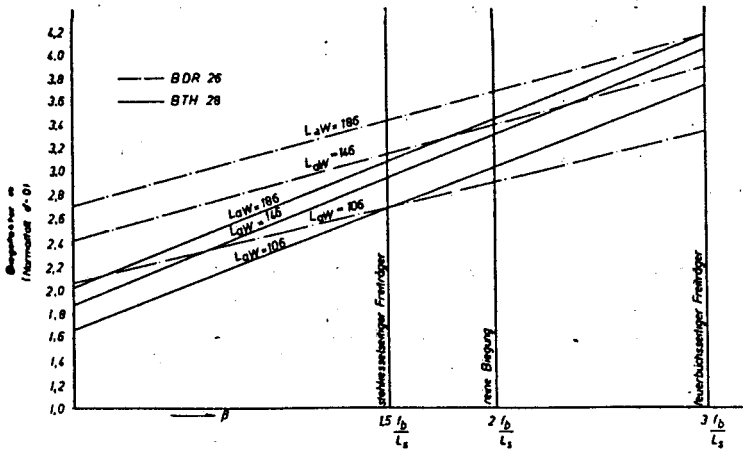

Abb. 12. Biegefaktor m bei BDR 26 und BTH 28 für L_{aW} = 106, 146, 186 mm (δ = 0)

The final value, the angle β, in the case of the symmetrical staybolts is further clarified in section 2. In the case of the firebox and also in the boiler the angles are equally large and in the case of pure bending are twice the number. The same conditions are applicable to the equalizing staybolts so that in the case of symmetrical staybolts there is always the same factor in those three special situations. Because of (71) and symmetrical staybolts the value m' becomes:

$$m' = m_{rB}$$

as well as $$m''_{rB} = 1 \qquad (73)$$

With the aid of the graphic determination according to the system of Mohr, one will also obtain in the event of same degree of bending, that is pure bending, the same value of the bend-direction (arrows) for the boiler and the firebox staybolts, which can be expressed in

$$f_{brB} = f_{bsF} + f_{bfF} \qquad (74)$$

The reasoning for this is based on the fact that each diameter is the sum of the bending momentums of two free-staybolts and is always equal to the bending momentum of a pure bending (compare Table1).

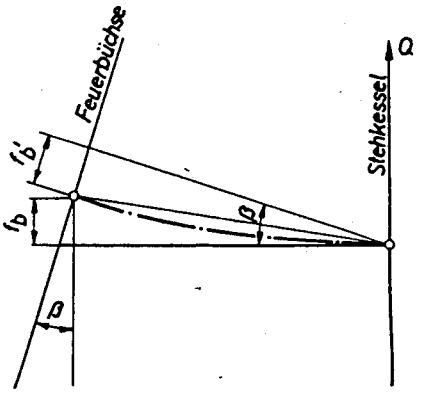

Abb. 13. Biegepfeile bei feuerbuchsseitigem Freiträger

With the graphic illustration of the bending lines for the free-carriers at or near the firebox side, according to the Mohrishe process one must consider that according to the Ill.13, the bending direction f'_b is not in agreement, which is needed for our calculations. The shift of f_b based on the drawing whose plane is on the main bending direction of the staybolts is in the distance of the plumline to the firebox side of the original axes of the staybolts. In the case of the boiler, the distance of free carriers is equal bending direction (arrow), but in the case of the firebox side it becomes f'_b as per (Ill. 13) of the indicated bending direction (arrow) and therefore is not in agreement with f_b. In order to obtain the true value of f_b, the elastic starting line of the power of Q, that is from the boiler side, must be applied. Also one can expect shifts of the bending directions in the case of nonsymmetrical staybolts with pure bending. Therefore, it is recommended in order to avoid errors that all elastic lines are drawn according to the process of Mohr in the boiler segment.

2) MATHEMATICAL TABULATIONS FOR THE DETERMINATION OF THE BENDING AND ANGLE FACTORS.

The exact determinations of these factors m, m' and m" is of significance, so that one can have error-free comparisons of the staybolts. For these reasons the Mohrishe Skyline system serves as the basis for the mathematical tabulations which will yield a satisfactory calculation for the accurate determinations of the factors.

As an example, using Table 1, the factors of BTH 28 L_{aW} = 146 mm representing the total length of the staybolt L_B = 160 mm, and the length of the shaft L_s = 126 mm (Ill.14) have been calculated. The staybolt is in Ill.14 between the two weldseams with a 10 mm width in Part I-XIV and a 6 mm width in Part XV used. The weldseams are as is commonly used 4 mm strong. The strengthening to 6 mm does not produce any important change in the bending factor.

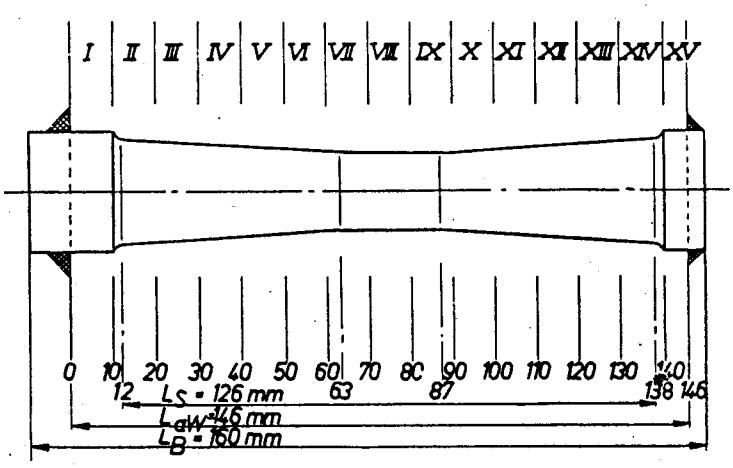

Abb. 14. Teilstücke I—XV zur Errechnung der Biege- und Winkelfaktoren m bzw. m′ nach dem Mohrschen Seilzugverfahren. Strichpunktiert: Änderungen des Querschnittsverlaufs (L_{aW} = 146 mm)

The mathematical tabulation and calculations of the bending angle factors for the three special cases is based on the determination of the bending and carrier moments for those in the middle of Part I-IV and the staybolts' diameters. If a break appears, that is a change in diameter which will only produce a further division in the two subparts for the purpose of calculations. As an example, this is the case with parts II, VII, IX, and XIV.

For the centers of the subparts one must first calculate the quotient M/J. The Table I is subdivided into four vertical groups. The Group I has I-V subgroups which contain all the special values of the special cases that correspond to l_{bss} in subgroup I with the diameter distance of the boiler site application. In Group II one finds the external diameter D which can be obtained either by the drawing or be mathematically exactly determined. Group III contains the width b of the individual part surfaces. This determines the effective width of the middle of the parts in conjunction with the bending momentum. As has been already mentioned above, this value in general is 10 mm; only in a part where the diameter is not consistent is it important that intermediate values be calculated or determined. At these points not only are the values of the breaking point but also the middle value for the remaining part entered. Note Table I as well as the dotted line in Ill. 14 indicating the plane of the break. Column 4 contains the resistance points W_B. In column 5 the carrier capacity J_B for the diameter D (column 2) the diameter needs calculations.

In the second Group II (columns 6-9) the free carrier of the boiler , and in the Group III (columns 10-13) for pure bending and in Group IV (columns 14-17) for the firebox, are the values, which are basic for the calculations to determine the diameter. One must determine the bending-momentum M_B with a bending power Q = 100kg to determine the quotient M_B/J_B. Therefore one can obtain the effective numbers for the partial plane as products $b(M_B/J_B)$, where b represents the width of the part.

Tabelle I Errechnung der Biege-, Winkel- und Vergleichsfaktoren m, m' und m'' für einen BTH 28, $L_B = 160$, $L_{aW} = 146$, $L_s = 126$, $L_{iW} = 120$, $l_k = 51{,}0$, $l_z = 24{,}0$ mm

I						II				III				IV			
1 Querschnittsabstand		2 Durchmesser	3 Wirkungsbreite	4 Widerstandsmoment	5 Trägheitsmoment	6	7	8	9	10	11	12	13	14	15	16	17
						stehkesselseitiger Freiträger				reine Biegung				feuerbuchsseitige Freiträger			
l_{bss}		D	b	W_B	J_B	M_B	M_B/J_B	Teilflächen-Inhalt $b \cdot \frac{M_B}{J_B}$	Σ	M_B	M_B/J_B	Teilflächen-Inhalt $b \cdot \frac{M_B}{J_B}$	Σ	M_B	M_B/J_B	Teilflächen-Inhalt $b \cdot \frac{M_B}{J_B}$	Σ
mm		mm	mm	mm³	mm⁴	mmkg	kg/mm³	kg/mm²	kg/mm²	mmkg	kg/mm³	kg/mm²	kg/mm²	mmkg	kg/mm³	kg/mm²	kg/mm²
0	stehk. seitiger Kopf	28,0	—	2 155	30 172	14 600	—	—	—	14 600	—	—	—	0	—	—	—
5		28,0	10	2,155	30 172	14 100	0,468	4,680	4,680	14 600	0,485	4,850	4,850	500	0,017	0,170	0,170
10		28,0	—	2 155	30 172	13 600	—	—	—	14 600	—	—	—	1 000	—	—	—
11	Übergang	26,25	2	1 777	23 370	13 500	0,578	1,156	—	14 600	0,625	1,250	—	1 100	0,047	0,094	—
12		24,5	—	1 442	17 700	13 400	—	—	—	14 600	—	—	—	1 200	—	—	—
16	stehkesselseitiger Konus	23,99	8	1 355	16 250	13 000	0,800	6,400	12.236	14 600	0,899	7,192	13.292	1 600	0,099	0,792	1,058
25		22,84	10	1 168	13 300	12 100	0,910	9,100	21,336	14 600	1,098	10,980	24,272	2 500	0,188	1,880	2,936
35		21,57	10	985	10 620	11 100	1,043	10,430	31,766	14 600	1,373	13,730	38,002	3 500	0,330	3,300	6,236
45		20,29	10	820	8 300	10 100	1,218	12,180	43,946	14 600	1,760	17,600	55,602	4 500	0,542	5,420	11,656
55		19,02	10	676	6 400	9 100	1,421	14,210	58,156	14 600	2,280	22,800	78,402	5 500	0,859	8,590	20,246
61,5		18,19	3	589	5 390	8 450	1,569	4,707	—	14 600	2,709	8,127	—	6 150	1,140	3,420	—
63	Zylindr. Schafftteil	18,0	—	573	5 153	8 300	—	—	—	14 600	—	—	—	6 300	—	—	—
66,5		18,0	7	573	5 153	7 950	1,541	10,787	73.650	14 600	2,831	19,817	106,346	6 650	1,290	9,030	32,696
75		18,0	10	573	5 153	7 100	1,378	13,780	87.430	14 600	2,831	28,310	134,656	7 500	1,453	14,530	47,226
83,5		18,0	7	573	5 153	6 250	1,211	8,470	—	14 600	2 ,831	19,817	—	8 350	1,620	11,340	—
87		18,0	—	573	5 153	5 900	—	—	—	14 600	—	—	—	8 700	—	—	—
88,5	feuerbuchseit. Konus	18,19	3	589	5 390	5 750	1,067	3,201	99,108	14 600	2,709	8,127	162,600	8 850	1,642	4,926	63,492
95		19,02	10	676	6 400	5 100	0,796	7,960	107,068	14 600	2,280	22,800	185,400	9 500	1,484	14,840	78,332
105		20,29	10	820	8 300	4 100	0,493	4,930	111,998	14 600	1,760	17,600	203,000	10 500	1,267	12,670	91,002
115		21,57	10	985	10 620	3 100	0,292	2,920	114,918	14 600	1,373	13,730	216,730	11 500	1,081	10,810	101,812
125		22,84	10	1 168	13 300	2 100	0,156	1,580	116,498	14 600	1,098	10,980	227,710	12 500	0,940	9,400	111,212
134		23,99	8	1 355	16 250	1 200	0,074	0,592	—	14 600	0,899	7,192	—	13 400	0,825	6,600	—
138	Übergang	24,5	—	1 442	17 700	800	—	—	—	14 600	—	—	—	13 800	—	—	—
139		26,25	2	1 777	23 370	700	0,030	0,060	117,150	14 600	0,625	1,250	236,152	13 900	0,595	1,190	119,002
140	feuerbuchseit. Kopf	28,0	—	2 155	30 172	600	—	—	—	14 600	—	—	—	14 000	—	—	—
143		28,0	6	2 155	30 172	300	0,010	0,060 (60%)	117,186	14 600	10,485	2,910 (60%)	237,898	14 300	0,475	2,850 (60%)	120,712
146		28,0	—	2 155	30 172	0	—	—	—	14 600	—	—	—	14 600	—	—	—
						$-\frac{7}{10}$ des Endgliedes:			1 117,126 82,030 1 035,096				1 924,912 — 166,530 1 758,382				807,786 — 84,284 723,502

$$m_{sI} = \frac{1\,035{,}096}{351{,}000} = 2{,}96 \qquad m_{rB} = \frac{1\,758{,}382}{530{,}000} = 3{,}32 \qquad m_{fF} = \frac{723{,}284}{179{,}000} = 4{,}04 \qquad m_{rB} = \frac{m_{fF} + 2\,m_{sF}}{3}$$

$$m'_{sI} = \frac{117{,}186}{35{,}39} = 3{,}32 \qquad m'_{rB} = \frac{237{,}898}{70{,}710} = 3{,}36 \qquad m'_{fF} = \frac{120{,}712}{35{,}390} = 3{,}41 \qquad = \frac{4.04 + 5{,}92}{3}$$

$$m''_{sI} = \frac{3{,}32}{2{,}96} = 1{,}12 \qquad m''_{rB} = \frac{3{,}36}{3{,}32} = 1{,}012 \qquad m''_{fF} = \frac{3{,}41}{4.04} = 0{,}834 \qquad = \frac{9{,}96}{3} = 3{,}32$$

In the last columns one finds the additions of the plane of the break for Parts I-XV for the boiler. In the case of a subpart of 10mm width, only 10mm has the additional count. In the additional columns 9, 13, and 17 is permitted. The values of these columns for the purpose of determining the bending direction (arrow) have to be added, otherwise the numbers would be too high. For these reasons, in dealing with the last horizontal column for the example provided, only 6mm width of the final part with only 60% of the determined part plane content is to be considered in the addition column.

The first horizontal columns are related to the staybolts' excess in the case of the reduced head length of 10mm (Part I) of the boiler side. The next two columns are only 2mm width with a broad and steep part. This steep rise is in consideration of the middle diameter with l_{bss}= 11mm. In the Part II with a l_{bss}= 10mm and up to l_{bss}= 20mm one will find an 8mm section of new design part; for these parts one can determine a middle diameter with l_{bss}= 16mm. For parts with an unbroken diameter one will obtain middle diameters with l_{bss}= 5, 25, and 35mm and even higher. Moreover, for parts with a broken diameter, the numbers of the middle diameter have to be determined independently. In

order to obtain the pure bending, number column 13, one has to add the values of the diameters of columns 9 and 17 in Table I. The values of the end parts are in column 9, 13, and 17 in the penultimate horizontal line l_{bss} = 143 mm plus the appropriate corresponding angles β are in relation to the inclination of the car of the tram according to the Mohrishe process.

Regarding the total value in the columns 9, 13, and 17, the end part surfaces with the full width of 10mm of the end parts, where 50% are to be subtracted because the inclination of the elastic line in the Mohrishe process begins with the center of gravity of the part surface in the ultimate section. Only the half of the bending direction (arrow) will be effective. As in the example of the Part XV, only 6mm instead of the 10mm, like in the Parts I-XIV, the addition is further increased to 40% in the 7/10 of the end part.

For the complete symmetric staybolt the table is much simpler. One needs only the column for the boiler side of the free carriers. In the case of the firebox carrier side, one needs to use only the part plane content of the boiler side by adding from below to above. The end parts are thereafter in all cases equal. The columns for the pure bending can be ignored since (72) ($m_{rB} = m'_{sf} = m'_{fF}$).

In order to calculate the bending and angle factors, using the same methods, the values for the cylindrical staybolts are determined, as in the example of the BgD28. These calculations are more simple than for the symmetrical staybolts since the expressions W_B and J_B are always equal and the intermediate points are not needed. In the lower part of Table I the values for the calculations for the bending and angle factors are determined where the numbers in the denominator are the values of the cylindrical comparable staybolts BgD28.

Moreover, the control-calculations for m_{rB} yield the same value. The calculated bending factors m according to the values for BTH28 are L_{aW} = 146m in Illustration 12.

3) THE EQUATIONS FOR SPECIFIC CASES

For the new design staybolts the formulas for the specific cases for the carrier momentum J_B are to be divided by the angle factors. For the carrier momentum one utilizes the momentum of the boilerside staybolts applications J_{BE}.

The angle β of the staybolt is determined with the bending momentum so that in the part the m of the bending momentum corresponds to BgD. The total correction for the angle β with new design staybolts is by comparison BgD is m'/m = m" (see eq 67). Accordingly all angles β are to be multiplied with a value m". Therefore the following equation for the specific is to be considered:

a) Boilerside Staybolts

where the value becomes (24) = $\dfrac{E_B \; J_B}{b'_{stk} \; s^3_{stk} \; E_{stk}}$

The momentum for the carrier capacity is replaced in the equation, instead of a/m in the case of new design staybolts.

Therefore, (50)

$$\beta = \frac{f_a}{L_s} \cdot \frac{\left(\frac{L_s}{2} + \frac{a}{m_{sF}}\right)}{\left(\frac{L_s}{3} + \frac{a}{m_{sF}}\right)} \cdot m''_{sF} \qquad (75)$$

and (51)

$$M_{B_{ss}} = \frac{E_B \; J_{BE}}{m_{sF} \; L_s \left(\frac{L_s}{3} + \frac{a}{m_{sF}}\right)} \cdot f_a \qquad (76)$$

(24a) becomes (76a)

$$a = \frac{E_B \; J_{BE}}{M_{Bss} \; m_{sF}} \cdot \gamma \qquad (76a)$$

and in solving the equation for f_a one obtains

$$f_a = \frac{M_{Bss} \; L_s^2 \; m_{sF}}{3 \, E_B \; J_{BE}} + L_s \cdot \gamma \qquad (77)$$

The first member corresponds to the bending direction (arrow) of a free carrier bolt, the second member relates to f_{wstk} of the outward ruling (f'_a[1]) which is a result of the welding at the boiler sight replacement leads to the angle γ. Only the first member of the staybolts bending, in the new design staybolts, will have an enlargement of m_{sf}. The part of the welding process of f_{wStk} of the outward ruling remains unchanged and is only dependent for M_{Bss}. The same is to be applied for the firebox side welding f_{wFb}, which is already considered with β.

b) Pure Bending

For pure bending derived from (55b) in the case of new design staybolts

$$\beta = \frac{f_a}{L_s} \cdot \frac{\left(L_s + \frac{a}{M_{rB}}\right)}{\left(\frac{L_s}{2} + \frac{a}{m_{rB}}\right)} \cdot m''_{rB} \qquad (78)$$

[1] Vlg. Abb. 21, 1 Aufsatz, S.261, Nov-Heit 51.

and according to (53)

$$M_{rB} = \frac{E_B \; J_{BE}}{m_{rB} \; L_s \left(\frac{L_s}{2} + \frac{a}{m_{rB}} \right)} \cdot f_a \tag{79}$$

for firebox staybolts equation (61) becomes

$$\beta = 3 \, \frac{f_a}{L_s} \cdot m''_{fF} \tag{80}$$

derived from equation (59)

$$M_{Bfs} = \frac{6 \, E_B \; J_{BE}}{m_{fF} \; L_s^2} \cdot f_a \tag{81}$$

4) THE SITUATION MOMENTUM AT THE APPLICATION

With the equations 75-81 the β and the M_B values for the three exceptions can be calculated and the momentum of application determined. In Illustration 15 the application momentum is shown for the BTH 28 by L_{aw} = 146mm. The method of drawing corresponds in the second application to the BgD 22 description.

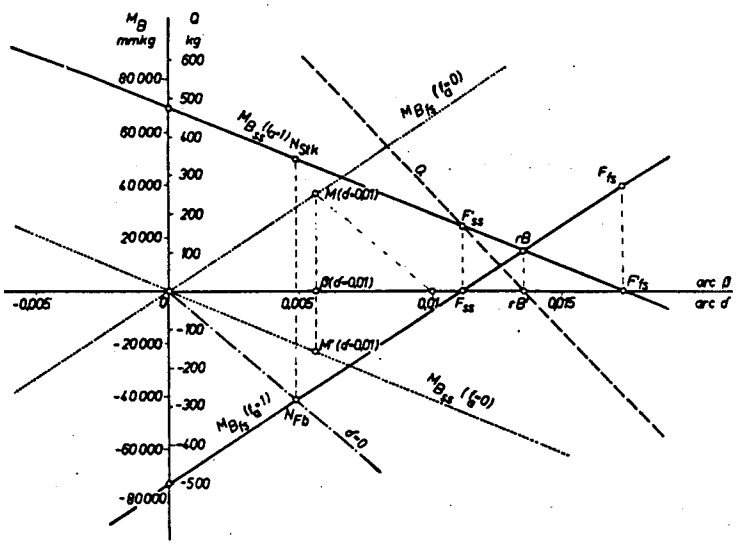

Abb. 15. Einspannmomentenbild eines BTH 28/18 bei L_{aW} = 146 mm, L_s = 126 mm (f_a = 1 mm)

All application momentums are similar and can be divided by the different situations of the special cases and the inclination of the application momentum lines. The distance of the vertical line through the points of F_{ss}, rB, and F_{fs} and therefore the difference of the of the angle β in the three cases of the new design staybolts is somewhat smaller than by BgD, since m" is in the case of the boiler staybolts >1, in the firebox carriers is <1. According to Illustration 15 indicates that the momentum with the positive δ are smaller

and ultimately with a pure bend a minimum is obtained. Negative δs in the case of new design staybolts are noted, then are the force momentums with BgD.

The lines of the force momentum for $f_a = 0$ are noted as parallels through the inclination point (Ill. 15 dotted line). An additional oblique position with $\delta = 0.01$ can be seen in the case of $f_a = 0$ at the firebox side force momentum $M(\delta = 0.01)$, the boiler force momentum $M'(\delta = 0.01)$, and the angle $\beta = 0.0056$.

5) THE PICTURE OF THE BENDING MOMENTUM

The picture of the bending momentum for BTH28 with $L_{aW} = 146$mm, $L_s = 126$mm as noted in Illustration 16. Also there is nothing of a basic new design principle. The calculated new design bending momentum lines are cut in the case of the new design staybolts points BS. The angles of β', β, δ, and γ all fall on a straight line. All definitions of Illustration 10 in the ninth segment of the second application are valid for the new design staybolts. As a result, in the case of staybolts with formed shafts with changing resistance momentum, the forces cannot be read directly from the picture of bending momentum.

The intersecting points of the lines of the bending momentum corresponding to the abscissa are also the turning points. For the calculated value $\delta = 0$ as an example, the turning point is with $l_{wfs} = 65.5$mm, and for $f_a = 0$, $l_{wfs} = 90.5$ (see Ill. 16).

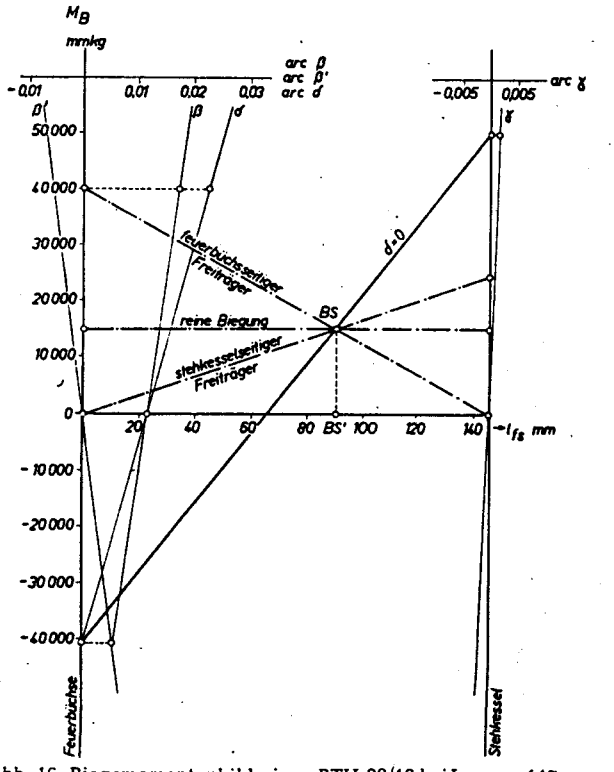

Abb. 16. Biegemomentenbild eines BTH 28/18 bei $L_{aW} = 146$ mm, $L_s = 126$ mm, ($f_a = 1$ mm)

6) THE RESISTANCE MOMENTUM PICTURE

For staybolts with new design shafts it becomes important to determine the force of the resistance momentum. Using Illustration 17 the resistance momentum for a BTH 28/18 considering the length of the staybolt can be noted. The perpendicular through the middle of the wall distance L_{aW} in this special case is not in the middle of the cylindrical part of the shaft, since the head of the boiler side is longer when compared to the firebox side. The middle horizontal part indicates the area of the cylindrical part of the shaft, following the curves of the area of new design, following the lines on both sides represents the new design part of the diameter of the head at the application point.

If one desires the approximate diameter for a certain situation, one needs to read only the turning point of the elastic line in Illustration 16 and consider the abscissa of Illustration 17. If one draws from this point a tangent to the most distant branch of the line of the resistance momentum (W_B-line) then the abscissa of the contact point gives the desired information. Also the tangent will give other values from the line of bending momentum. The force maximum of the diameter is given with M_B/W_B. If one takes the numerical difference of M_B and W_B as x, this then will yield the value of the contact point x kg/mm^2, since the contact point is in Illustration 17 $M_B=W_B$. However, in all other points the quotient is < x kg/mm^2 since the contact points according to the drawing is always WB>MB.

The pictures of the bending and resistance momentums are simple means to calculate. Staybolts with new design shafts and the characteristics of certain staybolts with particular demands can be checked. The less the contact is regarding the resistance momentum curve and the bending line, the more level shall be the force curve, the more equalizing the force and the less the force point.

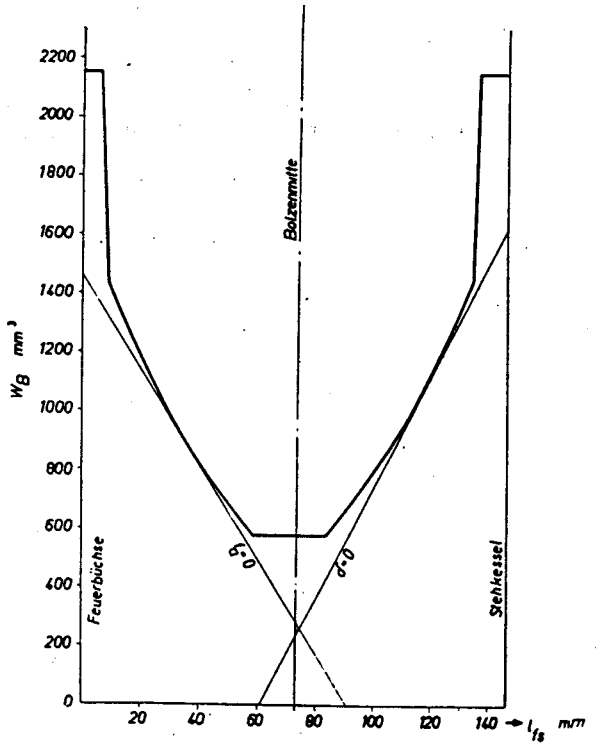

Abb. 17. Widerstandsmomentenbild eines BTH 28/18 bei L_{aW} = 146 mm, L_s = 126 mm mit Momentenlinien zur Bestimmung der gefährdeten Querschnitte

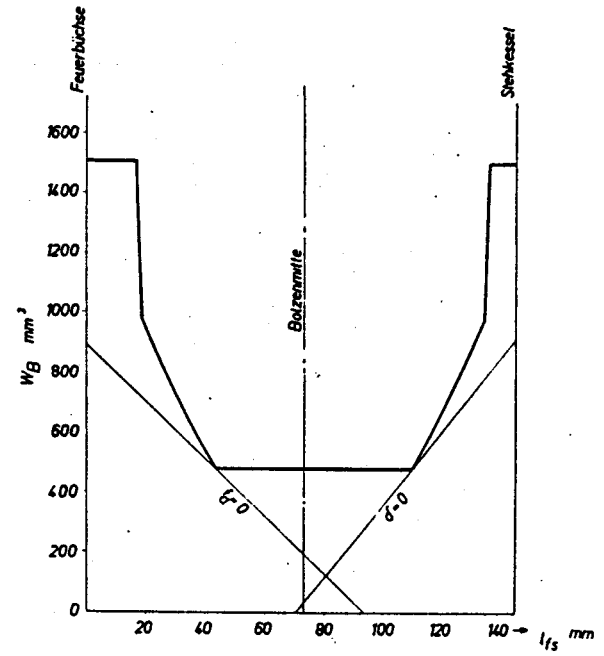

Abb. 18. Widerstandsmomentenbild eines BDR 26/17 bei L_{aW} = 146 mm, L_s = 126 mm mit Momentenlinien zur Bestimmung der gefährdeten Querschnitte

The pulling force in these cases has not been considered. This will, with decreasing shaft diameter in the middle of the shaft, increase. For this reason one should strive that the contact point in the upper part of the resistance curve momentum be as level as possible.

In Illustration 18 one can see the resistance momentum for a BDR 26 L_{aw} = 146. The particular diameter depends on a rather minimum length of the staybolt, upwards during the transition from a conical to a cylindrical part of the shaft and therefore will yield, with lengthening of the staybolt, an increasing force point which will further increase the tension force as can be noted in Illustration 21.

7) THE EFFECT OF TENSION FORCE

In all the previous considerations, of the second and this one, only the bending forces have been considered as these occur under various circumstances and conditions. Also one must add the tension forces as needed. Every staybolt has to endure the pressure of the boiler wall minus the smallest diameter of the shafts. The diameter of the shafts of the staybolt is expressed by $(\pi * D^2_z)/4$, where D_z corresponds to the cylindrical shaft diameter.

The force surface of the staybolt F_t is expressed by:

$$F_t = t^2 - \frac{\pi \cdot D_z^2}{4} \tag{82}$$

and the tension force by

$$P = p \cdot \left(t^2 - \frac{\pi D_z^2}{4} \right), \tag{83}$$

where p is the boiler pressure expressed in kg/mm^2.

The diameter of the staybolt is expressed in

$$\pi \cdot \frac{D^2 - d^2}{4} \Big), \tag{83a}$$

The values for D and d represent the external and internal diameters of any staybolt.

The tension force becomes

$$\sigma_z = \frac{4\, p \left(t^2 - \frac{\pi\, D_z^2}{4} \right)}{\pi\, (D^2 - d^2)} \tag{84}$$

The value of the tension force is not only dependent on the external and internal drilling diameter but also on the shaft diameter D_z. The change brought about by D_z is small in

relation to D_u in the case of a small shaft diameter where one can utilize equation (π * D^2_z)/4 of the relationship to t^2. In Illustration 19 the tension force δ_z is dependent on D_z with the drilling d = 6mm and the boiler pressure of p = 16 atmosphere.

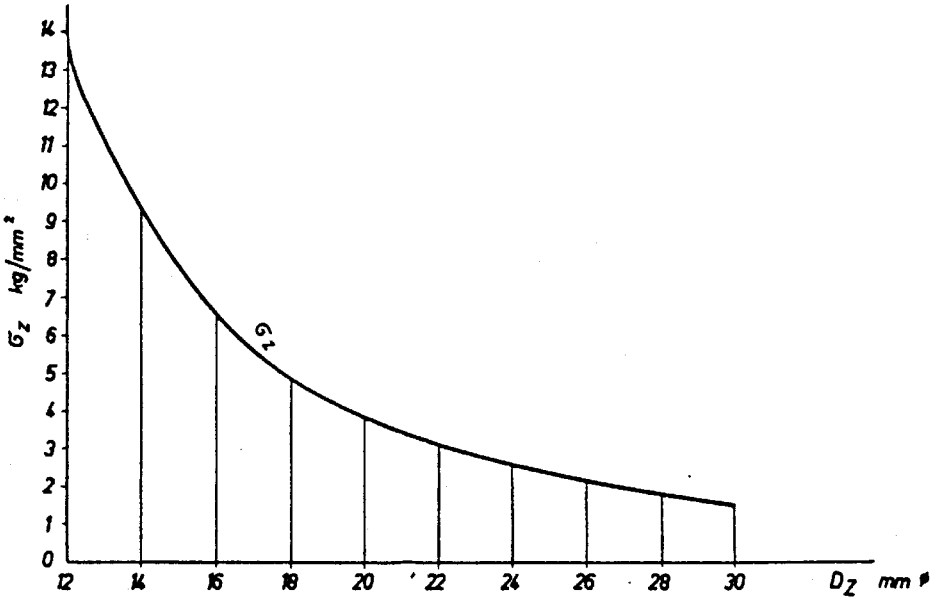

Abb. 19. Zugspannung σ_z in Abhängigkeit vom Bolzenschaftdurchmesser D_z für d_z = 6 mm bei t = 85 mm und p = 16 atü

8) THE INFLUENCE OF THE COMPRESSION AND EXPANSION

When staybolts are undergoing bending a shearing based on older types of calculations are expressed on the firebox side downward and in the boiler upward. Under that assumption the staybolts would in the case of the firebox exert a compression and in the boiler an expansion. However, based on newer knowledge, the firebox will undergo contraction while in use and the staybolts will in the majority, on the side of the firebox, bend downwards and also bend in the center part of the wall. Therefore the firebox under the shearing force will experience expansion and the boiler compression. Compression and expansion will yield a decrease in the bending direction (arrow) and consequently an easement on the staybolts. This diminuation of the bending direction becomes only then important if the shearing forces of the parallel and above lying staybolt values are added. According to the earlier conditions the firebox would be uniformly compressed and the boiler uniformly expanded. This yielded mathematical values which for the expansions and contractions are larger than f_{azul} and even more so in the case of bending which becomes larger that the anticipated value of f_{azul} depending on the shearing force.

With non-uniform additions of staybolts, as may be the case in the firezone, where mattress like situations may occur, one may encounter in part of the wall negative as well as positive shearing forces. The total compression and expansion values are contributing only in a small quantity. However if one is able to avoid a mattress like situation so that the staybolts are balanced, and the additional slanted positions at the edges (zones) follow as factors of measurements then mostly only the flexible staybolts are affected. The

compressions and expansions yield for the easement of the staybolts in the boiler which have been welded are of significance. According to the modern concepts of measurements of the bending of the staybolts one can anticipate that the shrinkage will be noted in the shape of rays in the direction of the hottest zone of the firebox below the fire arch. Compression and expansion diminishes shrinkage and the consequential bending direction will be more so depending on the degree of the shearing force.

In Table 2 one will find all the shearing forces are obtained by calculations when the staybolts have reached the limit of warm expansion, $\delta_z = 14$ kg/mm^2 and in the extreme part of the diameter as shaped by bending ($\delta = 0$) has occurred.

Tabelle 2
Querkräfte in kg

L_{aW} (mm)	106	146	186
BgD 18	89	67	54
BDR 26	216	103	68
BTH 28	336	235	182

The difference of the comparable staybolts is significant.

One considers an average length of the staybolts according to $L_{aW} = 146$ which will give compression and expansion with BTH 3.5 times the value than in the case of BgD. The front part in the case of BDR will be smaller depending on the length of the staybolt. A possible large force will give a diminishing of the bending of the staybolt.

9) TENSION CONDITIONS

With the aid of the second article and this article describing methods and formulations, one can consider Illustration 27 in the first article for BgD 18, BDR 26, and BTH 28. For the three the considered tension curves are calculated and the staybolts are graphed. With the aid of the bending and resistance momentum, the tension $\delta = 0$ and $f_a = 0$ are determined. In the case of both factors , the pulling tension according to Illustration 19, is added to the middle bending tension. When $\delta = 0$ the compression and expansion must also be considered.

10) THE BENDING OF THE STAYBOLTS IN THE PLASTIC AREA

Already in the segment D 1d for the first article[2] the bending of the staybolts in the plastic area has been examined and it has been pointed out that the steeper the tension point appears the shorter part of the edge is deformed plastically. The maximum strength is correspondingly larger.

Therefore on the basis of the calculations and measurements no doubt can exist that the staybolts during the process of welding and also during the larger part of the time they are progressively plastically bent. The calculated permissible values for bending f_{azul} are far

[2] S. 267/268 Nov.-Heft 1951

below the actual measured bending values. In the case of urgent necessity, the real wall effect can be minimized and the permissible value of f_{azul} is possible to enlarge but one will notice that it is nearly impossible to improve both values. One best avoids the plastic bending of the staybolts altogether.

The behavior of the staybolts in the plastic area is a key for the compression and understanding with different types of forms of the staybolts. This is best obtained through actual experience. This behavior will be considered in detail henceforth.

The formulas in the last and this article are only applicable for the plastic area. After surpassing the limits of the stretch, the bending momentum and the shearing forces do not follow a linear relation. The momentum and shear force curves begin to level out the more the staybolts are bent. At the extreme tension point the staybolt is bent at the cut of the diameter and its surroundings are further stretched to the overload. Such a local plastic stretch is expressed as a "plastic joint."

Using the tensile test it is well known with the tension-stretch diagram one will find that there will be one above and another below the limits of flow. The first is about 0.1% of the stretch value, from then on the power needed for further stretching is decreasing. Only after the stretch at 3% one once again commences the increase in strength which is noted in the increase in tension of the original crosscut.

In the event of the bending, the stretching of the exterior fiber in the plastic area through the support of the interior has not reached the limit of the stretch of the stretched fibers. The degree of support can be seen in Illustration 20a-c. At point A the tension of the side of the bending is reached by the limit of stretch which is 0.1. Thereafter the expression of the much larger diameter cut will yield a much larger support role. However if the stretching of the exterior fiber in the case of A exceeds 0.2% so will in the linear course the cut of the diameter proceed from the elastic to the plastic deformation, of the preformed area of the diameter cut and therefore to the value of 156%, in other words a 1.5 fold increase (Ill. 20c). In this case the tensile strength from the boiler pressure are not even considered and also the shift of the null-line to the side of the least yielding pressure side of the diameter. Considering the tensile stress the effective support will be largely diminished.

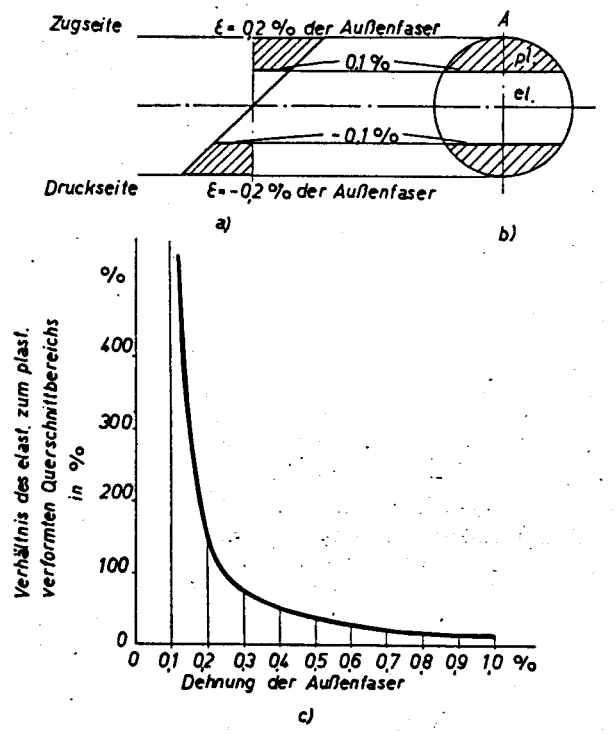

Abb. 20. Stützwirkung des inneren Querschnittsbereichs bei plastischer Beanspruchung der Außenfasern

In the hatched part of Illustration 20a and b the material is plastically deformed so no further increase in the bending power for further deformation is needed. With increasing bending of the staybolts the non-hatched part of the illustration for the diameter becomes progressively smaller. The resistance momentum of the remaining staybolts in the elastic stretched part of the diameter decreases rapidly.

As a consequence the effective support of the interior fibers commencing with the bending and deformation, begins only at the higher values of the bending direction as can be determined by calculations of the stretch at the edge fibers. Only when the stretch values of the edge fibers reaches 0.2- 0.3% one can observe a significant deformation. The power needed for further bending is not very significant. With the stretching of the exterior fibers to 3% begins the solidification of the material, that is, in the case where the bending is nearly the total diameter, exceeding the deformation.

The effective support must decrease as the strength of the exterior fiber increases and the stretching is augmented, and one should be prepared that the circular diameters with the strong tension point are only effective at and with an edge fiber stretch of 0.3%. Thereafter the diameter is to be considered a “plastic length.” With a 90 degree diameter the effective support will decrease because the relationship from the elastic to the plastic part of the diameter rapidly decreases in the case of the circular staybolt.

As long as the staybolt regarding the diameter is only used in the elastic phase, the effective stretch in the exterior fiber will be the effective tension. However, when the exterior fiber surpasses the limits of the stretch, one will note that the difference in the

plastic area in contrast to the elastic area becomes larger. The narrower part seen from the axial point, the area of the material contacts which are the limiting factors, that is particularly in the case of steep tension points, may be characteristic of some staybolts. In the case of the new designed staybolts approximately of equal tension in the exterior fiber the bending is distributed over the entire designed length. The staybolt should yield with the same bending power and the same bending direction but with smaller values.

The number n of the deformation change is one that under permanent demand of bending with the material will indicate the value that will hold until breakage decreases at several z values when $z = \frac{\varepsilon_1 \text{ max}}{\varepsilon_2 \text{ max}}$

That means that the maximum stretch of ε_1 of the local strongest stretch of staybolt 1 is related to staybolt 2 to ε_2 of the local staybolt. The force change relations n_2/n_1 shall be according to the curve of Wohler for the same relations to z. This will be depending on the demands of the staybolt 2, that is the permanent bending exchange tension. These thoughts depend on the results of vibrations and operational experiences.

For all the plastic deformed building material it becomes as uniform as possible to obtain the tension, something which is absolutely necessary for the exterior fibers. Otherwise one will obtain only a short, small part of deformation which will or may exceed the permissible values. This may in turn in the face of a small load produce a break that in turn will yield more corrosion, furthermore accelerating the process of breakdown. The exact determination of the tension in staybolts in the area of elasticity and the correct shape of the staybolt in the plastic area yield much more advantages than in the elastic area. The tension in the elastic area of the staybolt needs to receive the consideration for values of the plastic area.

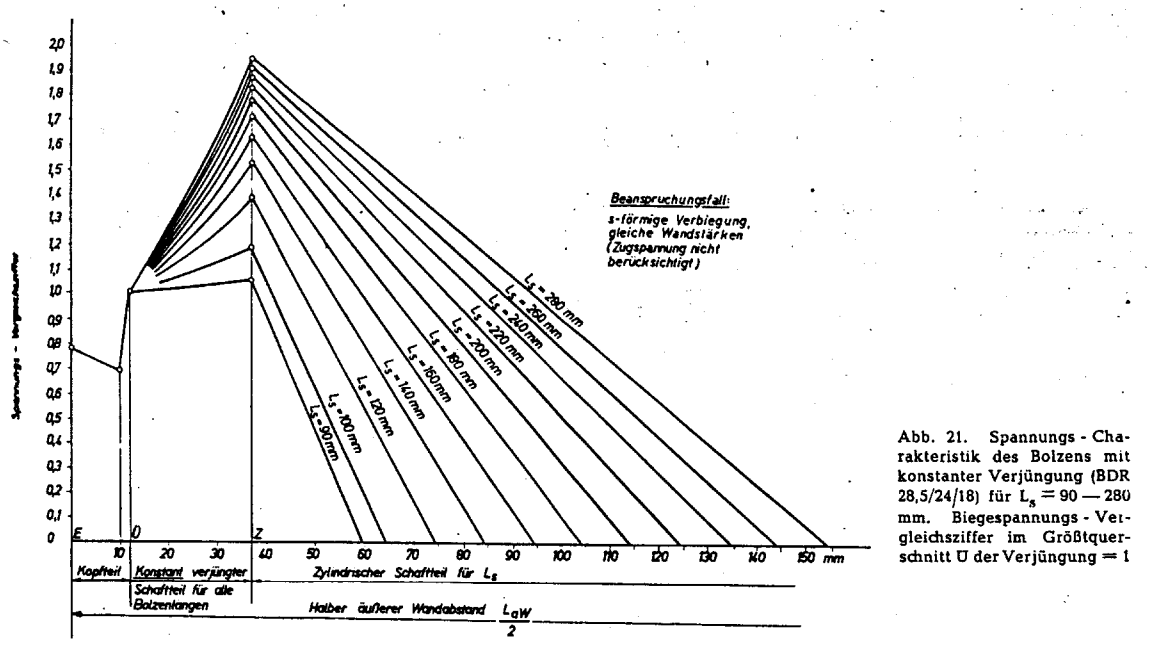

Abb. 21. Spannungs - Charakteristik des Bolzens mit konstanter Verjüngung (BDR 28,5/24/18) für $L_s = 90 — 280$ mm. Biegespannungs - Vergleichsziffer im Größtquerschnitt Ü der Verjüngung = 1

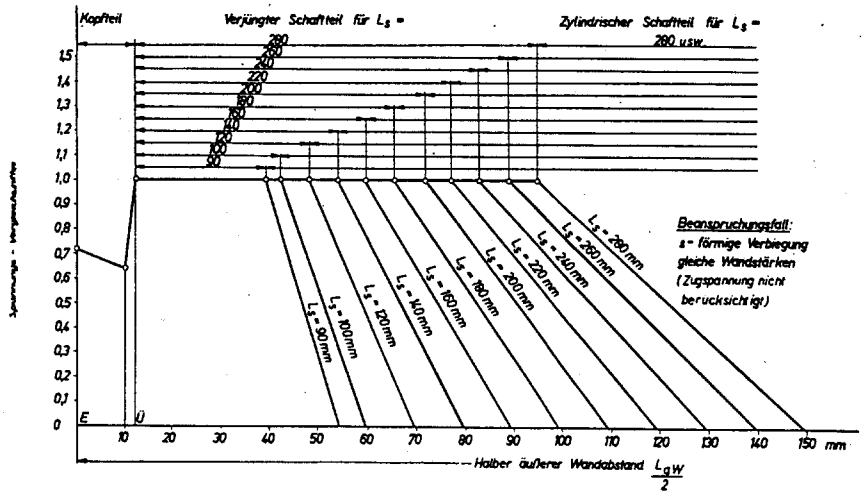

Abb. 22. Spannungs - Charakteristik des Bolzens mit für den gewählten Beanspruchungsfall spannungsgleicher Verjüngung (BgW 28,5/24.5/18) für L_s = 90 — 280 mm. Biegespannungs-Vergleichsziffer im Größtquerschnitt Ü der Verjüngung = 1

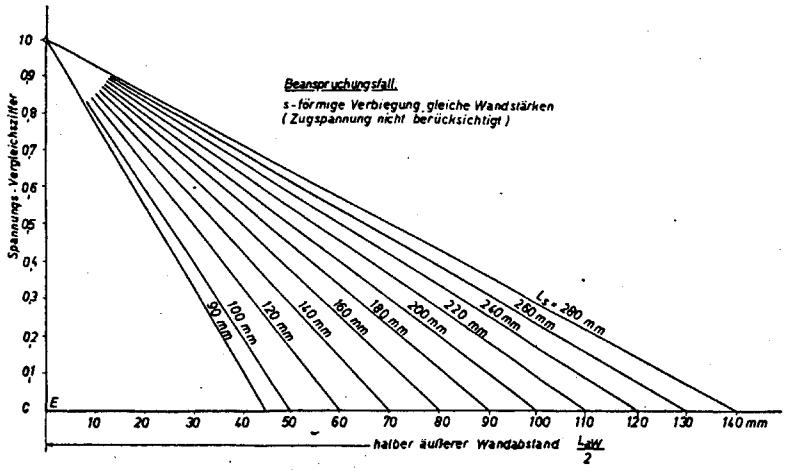

Abb. 23. Spannungs - Charakteristik des Bolzens mit gleichbleibendem Durchmesser (BgD 18) für L_s = 90 — 280 mm

For a better understanding of all the circumstances one can find in Illustration 21-23 that the tension conditions for the staybolts BDR 28, BTH 28, and BgD 18 and the half of all staybolts with a symmetrical s bending for the shaft lengths L_s from 90 to 280 mm are recorded. The shifting point, because of uneven wall strengths, uneven wall temperature, and the pull tension are not drawn in this schematic and therefore are not considered. The shifting point is elevated on the boiler side and is diminished on the firebox side of the tension point. The tension of the bend in the plane of U is the largest diameter of the new design part in Illustration 21 and 22 = 1. The tension values are therefore numbers of relationships.

In Illustration 21 the tension characteristics for a BDR with 24mm as the largest part and 18mm as the smallest part diameters for all lengths of the staybolts that are of the new design is illustrated in 22. That gives the conditions of the staybolt with bending resistance for an s-shaped symmetrical bend (BgW). In that case the calculations are applied to the new design part in such a manner that the bending tension is distributed over the entire bolt.

It is clear that the fundamentals of the boiler are important, this depending on the length of the staybolts BDR 28.5/18 always with the tension point, while in the process from the conical to the cylindrical part, which with the largest lengths of the staybolt may reach nearly twice the value of the tension. While the resistance of the staybolt (BgW 28.5/18) tension with new design part and the exterior fiber over the whole length is evenly applied and is in a constant relationship to the length of the shaft L_s with respect to the stretch.

In Illustration 23 the tension characteristic is shown for the same length of the staybolt as in Illustration 21 and 22 when a cylindrical diameter (BgD 18) is present. The tension of the tension diameter is equal to 1, selecting a large measurement in the ordinate axis to provide an equalization of the conditions.

Information regarding the absolute degree of the bending tension cannot be extracted from Illustration 21, 22, or 23. But they provide a clear picture of the demands in the plastic area with definite characteristics of the tension stretch conditions. In the elastic area one has to compare the shapes of the staybolts in the segment with the dominating staybolts.

In Illustration 24 are three staybolts used for comparison, BgD 18, BDR 26, and BTH 28 that illustrate the tensile strength from the influence of boiler pressure over the total length of the staybolts. One will note that the tensile strength of the diameter regarding the bending tension decreases within the central part of the shaft. While on the left branch the tension curve (Illustration 21) increases, that is the tension point of the diameter cut z is strengthened.

In the case of BTH the new design part is to be calculated in such a manner that in this area for those most frequent appearing demands with consideration of the strength of the wall and the tensile strength one will obtain a nearly level curve. These characteristics for the bending and pulling comes close for the BgW in Illustration 22.

With the knowledge of the far-reaching significance of the plastic deformation one can consider the steel firebox. And equally well the copper and monel staybolts can be considered. In the absence of a definite limit of stretch in the case of the above building materials and as opposed to steel, which undergoes cold deformation which yields immediate hardening, one will find that the difference between tension and stretch of that type of building material are much smaller than with steel. In addition one must consider the small E-model and therefore with smaller bending will give a higher tension as well as an increased corrosion. In the case of staybolts made from other material one will encounter a flat tension curve especially in highly demanding boilers with steel bolts that have an advantage.

To ascertain the correctness of all these theoretical concepts, not only concerning the staybolts, but also for all the plastic deformed building materials, which are at this time in experimental progress, these have shown to be correct. So far experimental results as they are available have been supporting all these calculations and concepts.

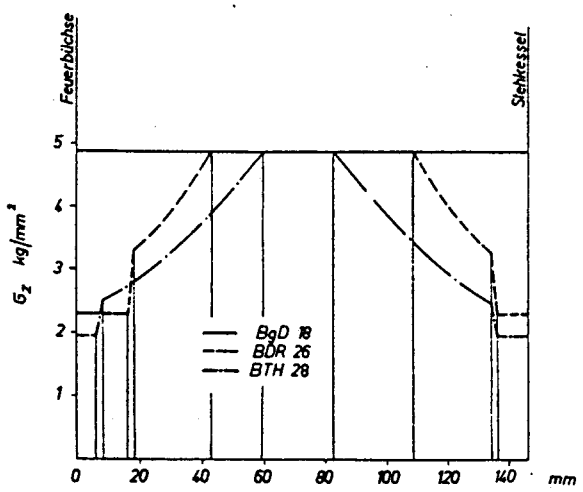

Abb. 24. Zugspannungsverlauf eines BgD 18, BDR 26/17, BTH 28/18 für L_{aW} = 146 mm, t = 85 mm und p = 16 atü

11) SUMMARY AND CONSEQUENCES

A process is discussed wherein all the possibilities for the staybolts with new design shafts, the bending momentum, the diameter force, the tension and deformation of the crosscuts under all kinds of demands are considered. For this purpose, the principles of the Mohrishe wire rope railway (suspension mountain system), a calculated and tabulated method for the determination of the bending and angle factors, where applied, as well as the three special cases of staybolts with new design shafts have been considered. With the aid of formulas the calculated values for the three special cases made it possible to obtain bending momentums, as well as tension values and other important numbers. With the aid of the resistance and bending momentums it is possible to generate a graphic display of the crosscuts that are at the greatest risk, as well as the tension for the remaining crosscuts. Moreover, for the normal s-shaped bending ($\delta = 0$), this process provides the possibilities for all the desired and needed numbers (values) to be obtained. Furthermore, with the staybolts one can evaluate the non-uniform strength of both walls as well as the uneven heating which will lead to the shift of the turning point under consideration of welding angles which will change with the tension momentum.

The described process permitted the graphic display of the tension diagrams for all types and kinds of new design staybolts. Therefore it is possible to select the most favorable form of the new design staybolts for whatsoever building demands may appear as well as the average case of the most favorable tension values.

The tension diagrams are most useful for the elastic area. Nevertheless, they have special meaning for the plastic area. This is the case with building materials where an upper and lower limit play a role in the stretching point in the plastic area. The higher and more difficult the tension point will be in the area of elastic. This knowledge shows clearly the excellent performance of the types of staybolt-forms BTH according to Table 1 and 2 in issue 12 of this publication (1951); in particular the characteristics of the copper and monel staybolts which undergo cold deformation, because of the absence of the stretch

limit and welding form. However, with the correct building shape, in the selection of other materials, significant performance and behavior in the plastic area are noteworthy.

In the elastic area the performance values and differences are smaller. From these understandings one can reach the following conclusions:

1) For staybolts, building material without limitations of the stretch capacity is preferable.
2) Steel staybolts perform best the more level the tension curve is, meaning the longer the level in the tension diagrams. For staybolts of copper, the shape of the shaft is of minimum importance when compared to the steel staybolt. When correctly measured the copper and KPS have advantages in the high demanding boiler.
3) Further improvements can be noted in the case of the s-shaped bending, if on the side of the firebox and the boiler approximately similar tension curves are found. Even very high-tension curves may be seen. Therefore the materials of the new design parts will have an optimal application.
4) Under these circumstances the boiler must undergo a diminishing of the boiler wall strength, so that in comparison to the firebox with diminished wall temperature, a higher elastic model is equalized. The difference between the strength of the wall and the temperature is expressed in the use of a non-symmetrical staybolt. Uneven wall strengths, uneven length of the head, and non-symmetrical new design parts all will shift the turning point. With additional differences the unequal parts which have been new designed can be used to calculate the boiler and firebox tension which should be nearly identical.
5) The diminishing of the strength of the boiler wall in relationship to the firebox strength wall yields greater advantages to the unsymmetrical staybolts, because one can decrease the burden in the boiler during the welding which is normally 16mm and in the firebox 10mm by a four fold. The boiler at least in the area of the rigid staybolts must be approximately 0.5-1.0 mm weaker than the firebox, which due to the differential heating of its' walls, are some changes in the elastic heating model resulting in equalization.
6) For each case there will be other optimal changes for the staybolts. Theoretically it would be possible by measurements of the bending lines, at each position, to utilize the most optimal staybolt. However if the similarity of the demands are very close one can delete the individual calculations and use the staybolts following the normal s-form.
7) Expansion and shrinkage of the firebox and the vaulted ceiling of the rear boiler give similar values for the s-form in the demands as needed. It is best that these demands are as similar as possible, in order to avoid additional conditions for the demands. In the case of the welded staybolts these aims have been reached as a rule, with the exceptions of the zones around the edges when dealing with boilers which have a vaulted sidewall. Therefore the area around the bulge, the mattress like construction, will avoid additional inclination. In the zones around the edges it is customary to use flexible staybolts whose utility will be discussed in a forthcoming publication.

ABBREVIATIONS AND OTHER EXPRESSIONS IN ALPHABETICAL ORDER

BgW = staybolt of same resistance for bending

b = effective width of a part when determining the bending and angle factors

D = exterior diameter of the staybolt

D_z = cylindrical shaft diameter

d = drilling diameter of the staybolt

F_t = loading surface of the boiler pressure for a staybolt

F_{bfF} = bending direction on the firebox side carrier

F_{brB} = bending direction in straight forward bending

f_{tbsF} = staybolt bending direction on the boiler side

L_{aW} = exterior wall distance

L_{iW} = interior wall distance

L_{bss} = distance of the staybolt crosscut from the boiler connection

m = bending factor

m_{fF} = bending factor on the side of the firebox

m_{rB} = bending factor in pure bending

m_{sF} = bending factor at the boiler carrier

m_n = bending factor in the normal case (δ=0)

m' = angle factor

m" = m'/m

J_{BE} = carrier momentum of the staybolt

P = boiler pressure